

## Vacuum thermal deposition of crystalline, uniform and stoichiometric CdS thin films in ambient H<sub>2</sub>S atmosphere

Beer Pal Singh<sup>a\*</sup>, Rakesh Kumar<sup>a</sup>, Ashwani Kumar<sup>b</sup>, Mahesh Kumar<sup>c</sup> & Amish G Joshi<sup>c</sup>

<sup>a</sup>Department of Physics, C C S University, Meerut 250 004, India

<sup>b</sup>Nanoscience Laboratory, Institute Instrumentation Centre, I I T Roorkee, Roorkee 247 667, India

<sup>c</sup>CSIR-National Physical Laboratory, New Delhi 110 012, India

*Received 23 March 2017; revised 3 May 2017; accepted 4 May 2017*

Crystalline, uniform and stoichiometric thin films of CdS have been fabricated on soda lime glass (SLG) substrates using vacuum thermal deposition method in the presence of hydrogen sulphide (H<sub>2</sub>S) atmosphere. The consequence of ambient H<sub>2</sub>S on the growth, quality and structure-property relationship of vacuum deposited CdS thin films has been investigated. The deposited films have been characterized by XRD, SEM with EDX analysis, AFM, XPS and optical spectroscopy. The physical characterization of as-deposited CdS films reveals that the films deposited in controlled H<sub>2</sub>S ambient are more crystalline, highly uniform and stoichiometric in comparison to films deposited without H<sub>2</sub>S atmosphere.

**Keywords:** Vacuum deposition, Stoichiometry, Cadmium sulphide, Hydrogen sulphide

### 1 Introduction

It is well recognized that the characteristics of thin films mainly depend on technique employed for deposition, nature of substrates, growth parameters, temperature and material doping. The structural, optical and electrical properties of deposited CdS thin films were mainly influenced by deposition conditions, e.g., deposition rate, substrate temperature and degree of vacuum<sup>1</sup>. Particularly, the effect of substrate temperature<sup>2</sup>, substrate rotation and deposition time<sup>3</sup>, optical band gap, refractive index, surface morphology and roughness of the vacuum evaporated CdS films have been studied. Recently, an intensive work has been carried out on the effect of coumarin additive<sup>4</sup>, Cobalt doping<sup>5</sup>, thermal annealing<sup>6,7</sup>, sulphide treatment<sup>8</sup>, growth temperature<sup>9-11</sup> and deposition time<sup>12</sup> on the properties of CdS films fabricated using various methods for numerous technological applications.

CdS is an important chemically stable II–VI compound semiconductor with a direct band gap of 2.4 eV. CdS thin films exhibits the significant interest for their potential application in various solid-state devices as solar cells<sup>13-21</sup> and gas sensors<sup>22,23</sup>. The numerous fabrication techniques have been employed for the deposition of CdS thin films such as

sputtering<sup>24-26</sup>, molecular beam epitaxy<sup>27,28</sup> (MBE), chemical bath deposition<sup>29-32</sup>, spray pyrolysis<sup>33</sup>, thermal evaporation<sup>3,9,34</sup>, PLD<sup>35,36</sup> and dip coating<sup>37,38</sup>. Among PVD, the vacuum thermal evaporation is an effective and inexpensive method for large area deposition thin films. Vacuum deposited thin film of compound semiconductors exhibited the lack of stoichiometry as the degree of dissociation due to thermal decomposition, strongly depends on the evaporation temperature and composition of the compound. Evaporation of compounds produces a gradient in the film composition because of evaporants are selectively vaporized, which adversely affects the quality and crystallinity of the thin film. Consequently, on the account of well-known fact that the stoichiometry in the films of compound semiconductors is a critical parameter that determines the properties and applications of the films in any device fabrication. This problem is an important issue in vacuum deposition of sulphide semiconductors because of their lower dissociation temperature. Due to elevated temperature of substrate the lighter sulphur ions get ejected from the substrate back into the vacuum chamber while the metallic ions were come across sulfurizing atmosphere (H<sub>2</sub>S) during their flight from vaporizing boat to the substrate. H<sub>2</sub>S is the well-known lightest sulfurizing gas and has more probability of encountering the metallic ions

\*Corresponding author (E-mail: drbeerpal@gmail.com)

and converts it back into compound sulphide before it strikes on the surface of the substrate. The process automatically maintains the stoichiometry and helps to produce the unit cell for the crystalline growth of the semiconductor thin films. The required small quantity of sulfurizing  $\text{H}_2\text{S}$  gas would be easily and safely produced in the vacuum chamber by thermal decomposition of sulfo-organic compound like thiourea and its isomer.

The vacuum thermally deposited thin films of compound sulphide semiconductors are non-stoichiometric and having deficiency of sulphur. The stoichiometry of the thin films was maintained using several techniques such as co-deposition of sulphur and sulphide semiconductor<sup>39</sup>, annealing the films with sulphide powder<sup>40</sup> and deposition of sulphide films in a controlled  $\text{H}_2\text{S}$  atmosphere<sup>41,42</sup>. Thermal decomposition of thiourea and its complex compounds is somehow a complex process which has been enormously studied experimentally and theoretically by various researchers<sup>43-45</sup>. Initially, thiourea starts to isomerize to ammonium thiocyanate ( $\text{NH}_4\text{SCN}$ ) at temperatures ranging from 140 to 180 °C and then in temperature range between 180-240 °C which produces main gaseous products like  $\text{CS}_2$ ,  $\text{NH}_3$ , and  $\text{H}_2\text{S}$  in both air and inert atmospheres<sup>45</sup>. Thermogravimetry, mass spectrometry and differential thermal analysis confirm the presence of  $\text{NH}_3$ ,  $\text{CS}_2$ ,  $\text{H}_2\text{S}$ , and  $\text{HNCS}$  gases<sup>43</sup>.

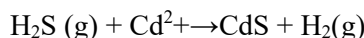
In the present study, the thermal decomposition of thiourea takes place in low pressure regime (inside the vacuum chamber). The gases having sulfurizing features would react with the present dissociated ions and rest of the gases would be sucked out using vacuum chamber. The other gaseous products like  $\text{CS}_2$ ,  $\text{HNCS}$  are unstable and would not be able to form the stable chemical compound with the heavier metallic ions. Therefore, the precise decomposition of thiourea would not significantly affect the stoichiometry of the deposited thin films.

The literature survey revealed that thiourea may be the best source of sulphur in chemistry based deposition of sulphide semiconductor films and has been extensively used by various researchers in the chemically deposited CdS films. To the best of our knowledge, none of the research group has been used thiourea as a source of sulphur in vacuum thermal deposition technique for the fabrication of sulphide semiconductors thin films. In the present work, we report an approach of using  $\text{H}_2\text{S}$  in vacuum thermal deposition of crystalline, uniform and stoichiometric

CdS thin films and the effect of  $\text{H}_2\text{S}$  ambient atmosphere on the growth and physical properties of the films.

## 2 Experimental Details

In this work, the thin films of CdS have been fabricated using thermal vacuum deposition technique on the glass substrates. To study the effects of  $\text{H}_2\text{S}$  atmosphere, thin films were deposited without and with  $\text{H}_2\text{S}$  atmosphere. High purity CdS powder (Sigma Aldrich, 99.99 %) was used for deposition and evaporated inside the vacuum chamber using molybdenum boat under  $\sim 10^{-5}$  torr pressure. Prior to deposition, the glass substrates were cleaned in acetone and washed in deionized water and iso-propyl alcohol (IPA). The distance between the molybdenum boat and the glass substrates was kept 12 cm inside the vacuum chamber. The films deposited in this way are nominated as 'CdS without  $\text{H}_2\text{S}$  atmosphere' right through in this manuscript. On the other hand, for the films deposited in the presence of  $\text{H}_2\text{S}$  atmosphere, the ambient  $\text{H}_2\text{S}$  atmosphere was achieved by controlled thermal decomposition of thiourea [ $\text{CS}(\text{NH}_2)_2$ ] in an electrically heated borosil test tube at about 150 °C inside the vacuum chamber.  $\text{H}_2\text{S}$  readily combines with the cations ( $\text{Cd}^{2+}$ ) without leaving any anions ( $\text{S}^{2-}$ ) at the substrates. The films deposited in this way are nominated as 'CdS with  $\text{H}_2\text{S}$  atmosphere' right throughout in the manuscript. Before deposition keeping the substrates at temperature ( $\sim 200$  °C) helps to eject out any sulfur atoms deposited during the thermal decomposition of CdS films. The higher reactivity of  $\text{H}_2\text{S}$  confirms a better conversion of the dissociated Cd ions into CdS and the stoichiometry maintained at every stage of the growth of the deposited film. The chemical reactions of thermal decomposition of CdS and  $\text{CS}(\text{NH}_2)_2$  and reaction of  $\text{H}_2\text{S}$  with Cd ions are as follows:



In decomposition of  $\text{CS}(\text{NH}_2)_2$  in a test tube,  $\text{H}_2\text{S}$  gas released inside the deposition chamber and solid residual product  $\text{CN}_2\text{H}_2$  gets deposited onto the cold portion of test tube and does not get away into deposition chamber in its free molecular state<sup>46</sup>.

The structural analyses of the samples were characterized using an X-ray diffractometer with

CuK<sub>α</sub> radiation. The surface microstructure and compositional analysis of the films were studied by scanning electron microscopy (SEM), atomic force microscopy (AFM) and energy dispersive X-ray (EDX). The chemical states of the films were investigated using an X-ray photoelectron spectroscopy, using a PHI 1257 model, operating at base pressure of  $\sim 1.3 \times 10^{-8}$  torr at 300 K with MgK<sub>α</sub> line at 1253.6 eV. Ultraviolet-visible spectroscopy analysis of films fabricated on the glass substrates has been investigated using Hitachi (U-3400) double beam spectrophotometer in the spectral range 350–850 nm at room temperature.

### 3 Results and Discussion

#### 3.1 Structural properties

Figure 1 shows the X-ray diffraction curves of both CdS thin films within the  $2\theta$  angle range from  $20^\circ$  to  $80^\circ$ . It can be clearly seen that the ambient H<sub>2</sub>S atmosphere causes a structural improvement and remarkably influences the crystallinity of vacuum deposited CdS films. Literature survey reveals that the CdS films can grow with hexagonal and cubic phase depending on several deposition parameters. Furthermore, the various researchers observed the phase transition from cubic to hexagonal due enhancing the substrate temperature or annealing<sup>47</sup>. Figure 1 shows that the ‘CdS film without H<sub>2</sub>S atmosphere’ exhibits a high intensity peak at  $2\theta$  value about  $26.52^\circ$  corresponding to (111) plane of cubic or (002) plane of hexagonal (JCPDS ICDD no. 80-0019) with the low intensity peak at diffraction angle ( $2\theta$ )

$48.11^\circ$  corresponding to (103) plane of hexagonal structure. While XRD pattern of vacuum evaporated CdS thin film fabricated with H<sub>2</sub>S atmosphere (Fig. 1, marked ‘b’) revealed that the significantly good crystallographic structure which is characterized by high intensity peak at  $2\theta$  value about  $26.52^\circ$  corresponding to (111) plane of cubic or the (002) plane of hexagonal (JCPDS ICDD no. 80-0006) with low intensity peak at  $2\theta$  value about  $48.11^\circ$  corresponding to (103) plane of hexagonal and at  $54.67^\circ$  corresponding to (222) plane of cubic or (004) plane of hexagonal phase. The peak positions of (111) and (222) planes of cubic structure are similar to the (002) and (004) planes of the hexagonal structure in CdS material. Therefore, it is difficult to conclude whether the deposited sample is purely cubic or purely hexagonal or mixture of these phases. The XRD pattern clearly revealed that both types of CdS films were polycrystalline in nature suggesting the hexagonal structure of both CdS films with preferential orientation along the (002) plane which is consistent with research work reported by Tomakin *et al.*<sup>10</sup> in CdS thin films, Donguk Kim *et al.*<sup>11</sup> in sputtered CdS thin films for solar cell applications and Ullrich *et al.*<sup>36</sup> in pulsed-laser deposited CdS thin film. However, in our experiment, an additional peak at  $54.67^\circ$  corresponding to (222) plane of cubic or (004) plane of hexagonal phase was induced by H<sub>2</sub>S atmosphere. Hence, it can be realized that vacuum evaporated CdS thin films deposited without and with H<sub>2</sub>S atmosphere are polycrystalline in nature and the H<sub>2</sub>S atmosphere significantly affects the crystallinity and growth of the CdS films. Furthermore, the intense and sharp peaks of CdS films deposited with H<sub>2</sub>S atmosphere are the consequence of highly crystalline nature of the deposited films without producing any contamination due to thermal decomposition of CS(NH<sub>2</sub>)<sub>2</sub> during the evaporation.

The crystallite size ( $t$ ) has been calculated using Scherrer formula<sup>48</sup>:

$$t = k \lambda / \beta \cos \theta \quad \dots (1)$$

where  $\beta$  is the full width half maximum (FWHM) of a particular diffraction peak in radians,  $\lambda$  is the wavelength used ( $\lambda = 1.5406 \text{ \AA}$ ),  $k$  is shape factor equal to 0.9 and  $\theta$  is the Bragg angle. The crystallite size of CdS films for without and with H<sub>2</sub>S atmosphere was estimated using (111) preferential orientation and came out 24.67 and 28.93 nm, respectively.

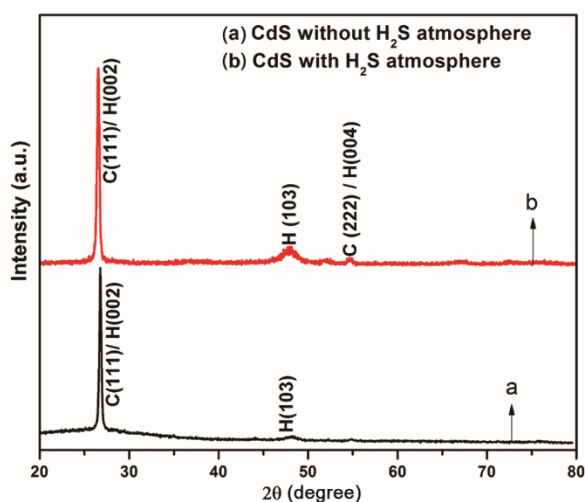


Fig. 1 — XRD patterns of vacuum evaporated CdS thin films deposited without and with H<sub>2</sub>S atmosphere

### 3.2 Surface morphology

Figure 2(a,b) shows the FE-SEM surface microstructure of vacuum evaporated CdS films fabricated with and without H<sub>2</sub>S atmosphere. As shown in Fig. 2(b), it is clear that the presence of H<sub>2</sub>S atmosphere during film deposition affects the surface microstructure and homogeneity of the vacuum thermal deposited CdS films. Therefore, it clearly revealed that the CdS films deposited without H<sub>2</sub>S atmosphere exhibit rough surface and the grains are not distributed uniformly. However, the CdS film deposited with H<sub>2</sub>S atmosphere depicts the fine grains which are more crystalline and almost uniformly distributed over the surface. Thus, the films deposited in H<sub>2</sub>S atmosphere are more homogeneous, dense and exhibit nearly crack free surface of the CdS thin film. As a result, it may be concluded that the improved surface morphology has been found in the CdS films deposited in controlled H<sub>2</sub>S atmosphere to enhance their performance in solid-state devices. Figure 2(c, d) shows the EDAX spectrum of both CdS films deposited without and with H<sub>2</sub>S atmosphere. The atomic % of Cd and S in respective film analyzed by EDAX is shown in the inset table of Fig. 2(c, d). The average atomic percentage of Cd and S shows excess of Cd in the vacuum evaporated CdS thin films without H<sub>2</sub>S atmosphere. These results indicate that the CdS films deposited with H<sub>2</sub>S atmosphere have better stoichiometry in comparison to CdS films deposited without H<sub>2</sub>S atmosphere.

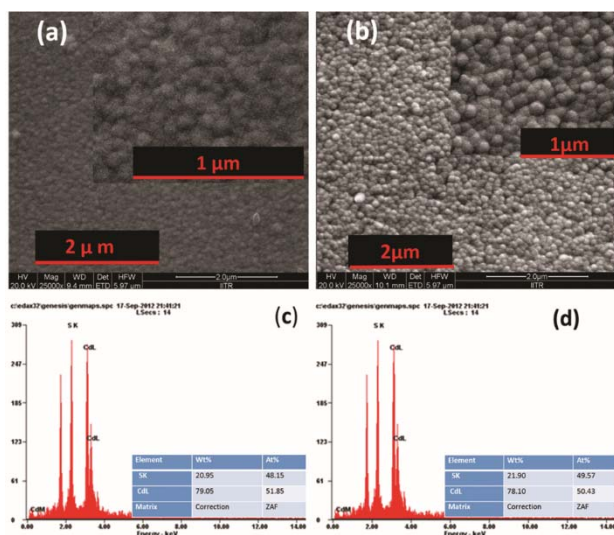


Fig. 2 — SEM micrograph of vacuum evaporated CdS thin film deposited (a) without and (b) with H<sub>2</sub>S atmosphere. The magnified images are shown inset. EDAX spectrum of vacuum evaporated CdS thin film deposited (c) without and (d) with H<sub>2</sub>S atmosphere

The 2D and 3D AFM topography with histogram distribution of vacuum deposited CdS thin films without and with H<sub>2</sub>S atmosphere are shown in Fig. 3(a, b), respectively. Here, the AFM micrographs of the CdS films fabricated with H<sub>2</sub>S atmosphere depicted that all nano grains were homogeneously distributed and spherical in shape over the whole film surface in comparison to the CdS films deposited without H<sub>2</sub>S atmosphere. The average crystallite size was found to be enhanced in CdS films deposited with H<sub>2</sub>S atmosphere. This result is in good agreement with the FE-SEM and XRD results. The average grain size and roughness of CdS films deposited without and with H<sub>2</sub>S atmosphere was found to be (12 nm, 2.39 nm) and (65 nm, 12.11 nm), respectively. Therefore, the average grain size and roughness of the CdS film deposited in controlled H<sub>2</sub>S atmosphere were found to be increased. Furthermore, AFM topography of CdS film with H<sub>2</sub>S atmosphere clearly reveals the cluster of particles with greatly compact structure and improved surface, which is well consistent with XRD and SEM studies.

### 3.3 X-ray photoelectron spectroscopy (XPS) study

Figure 4(a) shows the XPS survey scan spectra of vacuum evaporated CdS films deposited without and with H<sub>2</sub>S ambient atmosphere acquired in the energy range of 0-1150 eV. During photoemission studies, small specimen charging was detected and eliminated by grounding the sample and also calibrated by assigning the C 1s signal at 285 eV. Few peaks are impurity peaks which are marked with (\*). Both samples show the relatively sharp peaks of C 1s (285 eV), O 1s (532 eV), Cd (3d<sub>5/2</sub>), and Cd (3d<sub>3/2</sub>) at 405 and 412 eV, respectively.

The core level XPS spectra of Cd, C, S and O have shown symmetric profiles depicting uniform bond structure and emphasize that with and without H<sub>2</sub>S atmosphere exist in same phase. The core level spectra Fig. 4(b) of Cd (3d) shows two distinct Cd(3d<sub>5/2</sub>) and Cd(3d<sub>3/2</sub>) states for the same without CdS at 405.65 and 412.4 eV and while with H<sub>2</sub>S it shows the peaks at 405.35 and 412.15 eV, respectively. The Cd (3d) core-level XPS spectrum (Fig. 4(b)) is in well agreement with published values<sup>14,49</sup> for CdS. The separation of the states in without and with H<sub>2</sub>S atmosphere is 6.75 and 6.8 eV, respectively, which is due to spin-orbit splitting. The slight shift in the respective binding energies is due to variation from site to site substitution H<sub>2</sub>S gas. Figure 4(d) shows S (2p) and 2S (2s) core level spectra. The peaks with and without H<sub>2</sub>S atmosphere

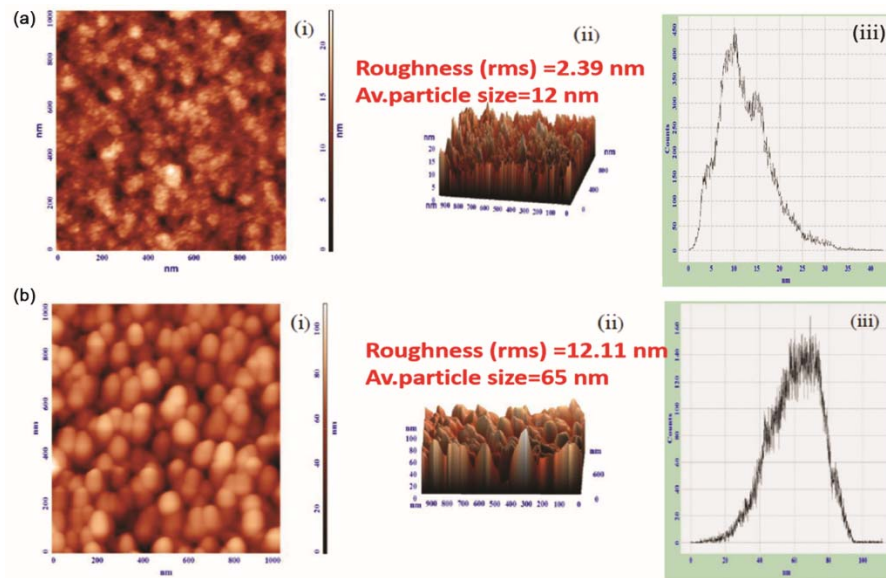


Fig. 3 — AFM images (i) 2D, (ii) 3D and (iii) Histogram distribution of vacuum evaporated CdS thin films deposited (a) without and (b) with H<sub>2</sub>S atmosphere

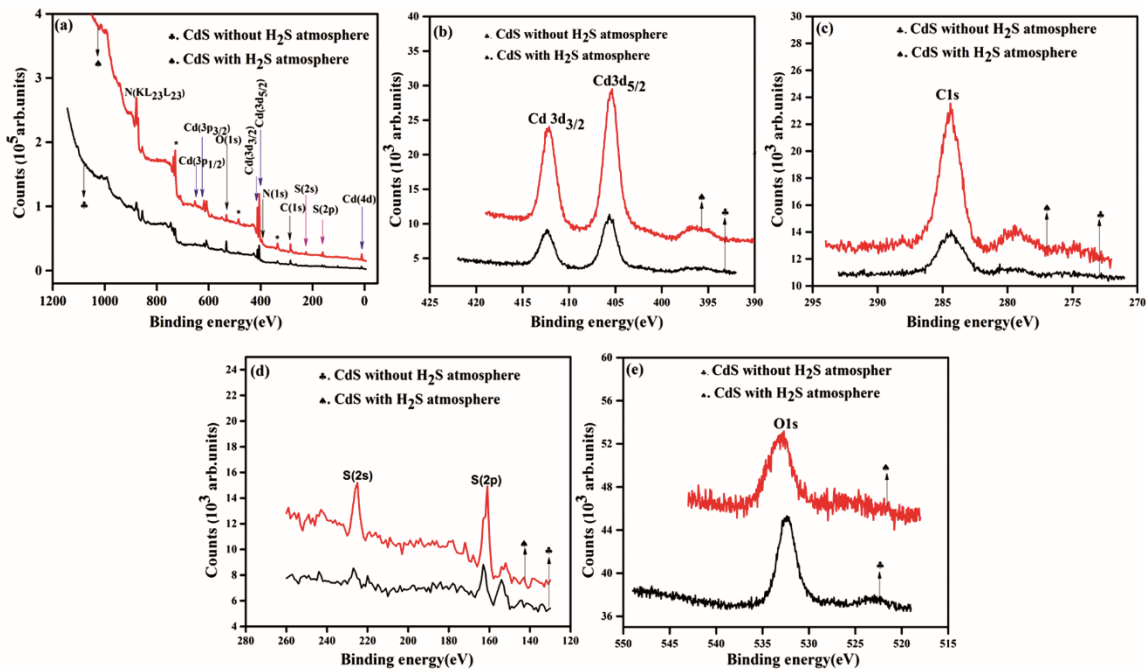


Fig. 4 — (a) XPS survey scan spectra of vacuum evaporated CdS thin film deposited without and with H<sub>2</sub>S atmosphere Core level XPS spectra of (b) Cd 3d (c) C 1s (d) S (2p & 2s) and (e) O 1s, vacuum evaporated CdS thin films deposited without and with H<sub>2</sub>S atmosphere

are observed that sulfur contributions is increased with H<sub>2</sub>S atmosphere CdS films. Fig. 4(e) shows O (1s) core level spectra. The peaks with and without H<sub>2</sub>S atmosphere are observed at 532.75 and 532.3 eV are the contributions from surface oxygen of CdS films.

The observed C (Fig. 4(c)) and O (Fig. 4 (e)) peaks can be attributed to the adsorption of these

elements on the surface of the microstructure due to the exposure to the atmosphere. It is clearly seen from survey scan spectra and core level spectra of CdS thin films that after introducing H<sub>2</sub>S atmosphere the films are indicating better stoichiometry condition, better crystallinity and growth in compared to without H<sub>2</sub>S atmosphere. This is

manifested by an increase in the Cd (3d) and S (2p) peak in survey scan spectra.

### 3.4 Optical properties

Figure 5 shows that the optical absorption coefficient increases significantly in 'CdS films with H<sub>2</sub>S atmosphere' (Fig. 5, spectrum marked 'b') whereas the absorption edge is at about same wavelength in both films. More and sharper absorption in 'CdS films with H<sub>2</sub>S atmosphere' than 'CdS films without H<sub>2</sub>S atmosphere' indicates that there are fewer defects and pin holes in the 'CdS films with H<sub>2</sub>S atmosphere'. This increment in absorption coefficient in 'CdS films with H<sub>2</sub>S atmosphere' is also due to increased volume fraction of CdS clusters as evident from SEM and AFM images. Fewer defects reduce surface scattering and grain boundary scattering which is favorable in improving the performance of any optoelectronic device.

Figure 6 depicts the transmittance spectra of both CdS films in the wavelength range 300-850 nm. Figure 6 revealed that both films exhibits very low transmittance below 450 nm, which is due to strong absorption in this wavelength regime. Thereafter, the transmittance increases (greater than 70 % in visible range) with increasing wavelength and shows an interference pattern towards higher wavelength, which is in well agreement with the results reported by various workers related to CdS films deposited by PVD techniques<sup>3,9,11,36,41,50,51</sup>. The presence of interference fringe in thin films is due to multiple reflections occurs at film/air and film/substrate interface. These reflections in films come into view with smooth

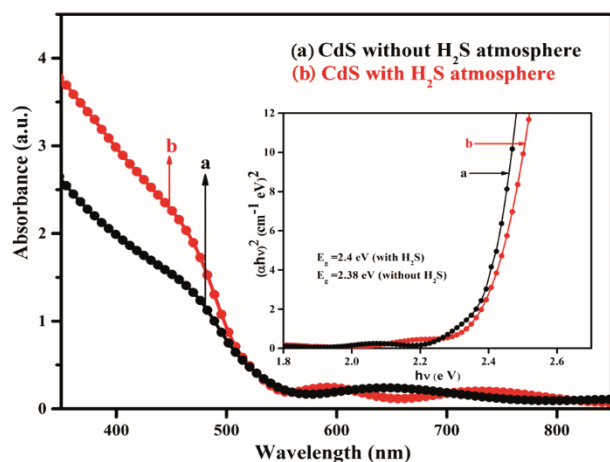


Fig. 5 — Absorption spectra of vacuum evaporated CdS/glass thin films deposited without and with H<sub>2</sub>S atmosphere. Inset shows the plot of  $(\alpha hv)^2$  versus  $hv$  for determination of optical band gap of films

surface and required thickness of the films. Moreover, the rough surface of the film has additional light scattering centers at the surface which results to reduce the number of interference fringes<sup>9</sup>. Therefore the more number of interference fringes in 'CdS films with H<sub>2</sub>S atmosphere' is in accordance with the film smoothness and thickness. The optical transmission spectrum of 'CdS film with H<sub>2</sub>S atmosphere' (Fig. 6, spectrum marked 'b') shows a sudden fall of transmission near the band edge which is an indicative of good crystallinity<sup>50</sup>. It can be observed that the films deposited in H<sub>2</sub>S atmosphere reveal good transmittance of about 78% and depict the steeper absorption edge which is the consequence of the good homogeneity in the distribution of CdS film composition.

The optical energy band gap of these films for both the samples was calculated with the help of absorption spectra (Fig. 5) using the following Tauc relation<sup>52</sup>:

$$\alpha hv = A(hv - E_g)^n \quad \dots (2)$$

where  $\alpha$  is absorption coefficient,  $A$  is constant,  $hv$  is incident photon energy,  $E_g$  is the energy band gap of the material and  $n$  depends on the nature of the material transition like  $n = 1/2$  and  $n=2$  for allowed direct and indirect transitions, respectively. Here, we used  $n=1/2$  for allowed direct transitions. The optical band gap ( $E_g$ ) values of 2.38 eV and 2.40 eV for CdS films without and with H<sub>2</sub>S atmosphere were calculated by extrapolating the linear portion of  $(\alpha hv)^2$  versus  $hv$  (Fig. 5) for direct transition in CdS compound which has been found in good agreement with the  $E_g$  values reported in the literature<sup>3,17,36,50</sup>. The slightly higher value of the optical band gap was obtained for CdS

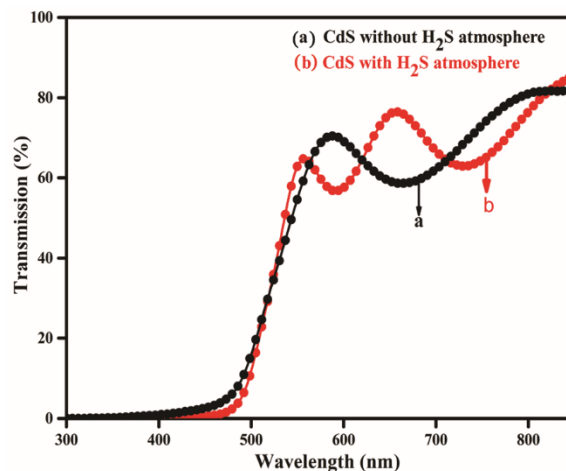


Fig. 6 — Transmission spectra of vacuum evaporated CdS/glass thin films deposited without and with H<sub>2</sub>S atmosphere

films deposited in H<sub>2</sub>S atmosphere, may be attributed due to the more stoichiometric composition of CdS films in comparison to CdS films deposited without H<sub>2</sub>S atmosphere. The thickness of as-deposited films was calculated using the spectroscopic method (envelop method) from transmission spectra (Fig. 6) using following relation:

$$t = \frac{M\lambda_1\lambda_2}{(2[n(\lambda_1)\lambda_2 - n(\lambda_2)\lambda_1])} \dots (3)$$

where  $M$  is the number of the oscillations between the two extremes,  $\lambda_1$ ,  $n(\lambda_1)$  and  $\lambda_2$ ,  $n(\lambda_2)$  are the corresponding wavelength and the indices of refraction. The film thickness of CdS with H<sub>2</sub>S and without H<sub>2</sub>S atmosphere has been found 428 and 416 nm, respectively. The spectroscopic method using transmission characteristics employed for the thickness measurement average out the variation of large area films thickness.

#### 4 Conclusions

In this study, uniform, crystalline and stoichiometric CdS thin films were successfully fabricated on the glass substrates using vacuum thermal evaporation technique. The effect of controlled H<sub>2</sub>S atmosphere on the growth and physical properties of the CdS thin films was studied. It is observed that the CdS films fabricated with H<sub>2</sub>S ambient atmosphere show dark orange color, more adherent and more uniformity as has been inferred by the sharpness of absorption spectra. Their transparency is also better than that of the films deposited without H<sub>2</sub>S atmosphere. X-ray diffraction curves of both films depicted that they have hexagonal structures oriented along the (002) plane. It is concluded that the films fabricated in H<sub>2</sub>S ambient atmosphere have better stoichiometry ratio and better crystallinity with improved smooth surface. Therefore, the characteristics of vacuum deposited CdS films deposited with H<sub>2</sub>S ambient atmosphere would be inherently more appropriate and favorable for any device fabrication.

#### Acknowledgement

The authors gratefully acknowledge the support from the UGC, New Delhi, Department of Physics, C C S University, Meerut (UP), India, Institute Instrumentation Centre, I I T Roorkee, India and NPL, New Delhi, India to carry out this research work.

#### References

- 1 Tyagi R C & Kumar R, *Thin Solid Films*, 25 (1975) S21.
- 2 Pal U, Silva-González R, Martínez-Montes G, Gracia-Jiménez M, Vidal M A & Torres S, *Thin Solid Films*, 305 (1997) 345.
- 3 Castro R R, Mendez G J, Perez Q I & Medina E R, *Appl Surf Sci*, 257 (2011) 9480.
- 4 Yücel E & Kahraman S, *Ceram Int*, 41 (2015) 4726.
- 5 Mukherjee A, Fu M, Ghosh P & Mitra P, *Mater Lett*, 141(2015) 39.
- 6 You C F, Lin Y J, Liu C J & Wu C A, *J Lumin*, 146 (2014) 109.
- 7 Ghosh B, Kumar K, Singh B K, Banerjee P & Das S, *Appl Surf Sci*, 320 (2014) 309.
- 8 Lin Y J, You C F, Chang H C, Liu C J & Wu C A, *J Lumin*, 158 (2015) 407.
- 9 Jaber A Y, Alamri S N, Aida M S, Benghanem M & Abdelaziz A A, *J Alloys Compd*, 529 (2012) 63.
- 10 Tomakin M, Altunbaş M, Bacaksiz E & Çelik Ş, *Thin Solid Films*, 520 (2012) 2532.
- 11 Kim D, Park Y, Kim M, Choi Y, Park Y S & Lee J, *Mater Res Bull*, 69 (2015) 78.
- 12 Garcia L V, Mendivil M I, Garcia Guillen G, Aguilar Martinez J A, Krishnan B, Avellaneda D, Castillo G A, Das Roy T K & Shaji S, *Appl Surf Sci*, 336 (2015) 329.
- 13 Zhao H, Farah A, Morel D & Ferekides C S, *Thin Solid Films*, 517 (2009) 2365.
- 14 Su Y W, Ramprasad S, Han S Y, Wang W, Ryu S O, Palo D R, Paul B K & Chang C H, *Thin Solid Films*, 532 (2013) 16.
- 15 Pérez-Hernández G, Pantoja-Enríquez J, Escobar-Morales B, Martínez-Hernández D, Díaz-Flores L L, Ricardez-Jiménez C, Mathews N R & Mathew X, *Thin Solid Films*, 535 (2013) 154.
- 16 Britt J & Ferekides C, *Appl Phys Lett*, 62 (1993) 2851.
- 17 Nazir A, Toma A, Shah N A, Panaro S, Butt S, Sagar Ru R, Raja W, Rasool K & Maqsood A, *J Alloys Compd*, 609 (2014) 40.
- 18 Lal C & Jain I P, *Int J Hydrogen Energy*, 37 (2012) 3792.
- 19 Guillén C, Martínez M A, Maffiotte C & Herrero J, *J Electrochem Soc*, 148 (2001) G602.
- 20 Repins I, Contreras M A, Egaas B, DeHart C, Scharf J, Perkins C L, To B & Noufi R, *Prog Photo Res*, 16 (2008) 235.
- 21 Han J, Spanheimer C, Haindl G, Fu G, Krishnakumar V, Schaffner J, Fan C, Zhao K, Klein A & Jaegermann W, *Sol Energy Mater Sol Cells*, 95 (2011) 816.
- 22 Senthil K, Mangalaraj D, Narayandass S K & Adachi S, *Mater Sci Eng B*, 78 (2000) 53.
- 23 Levinson J, Shepherd F R, Scanlon P J, Westwood W D, Este G & Rider M, *J Appl Phys*, 53 (1982) 1193.
- 24 Das N S, Ghosh P K, Mitra M K & Chattopadhyay K K, *Physica E*, 42 (2010) 2097.
- 25 Chandra S, Pandey R K & Agrawal R C, *J Phys D Appl Phys*, 13 (1980) 1757.
- 26 Lee J H & Lee D J, *Thin Solid Films*, 515 (2007) 6055.
- 27 Choi J W, Bhupathiraju A, Hasan M A & Lannon J M, *J Cryst Growth*, 255 (2003) 1.
- 28 Brunthaler G, Lang M, Forstner A, Giftge C, Schikora D, Ferreira S, Sitter H & Lischka K, *J Cryst Growth*, 138 (1994) 559.
- 29 Yao P C & Chen C Y, *Thin Solid Films*, 579 (2015) 103.
- 30 Cao M, Sun Y, Wu J, Chen X & Dai N, *J Alloys Compd*, 508 (2010) 297.
- 31 Lee T Y, Lee I H, Jung S H & Chung C W, *Thin Solid Films*, 548 (2013) 64.

- 32 Yücel E, Güler N & Yücel Y, *J Alloys Compd*, 589 (2014) 207.
- 33 Ravichandran K & Philominathan P, *Appl Surf Sci*, 255(2009) 5736.
- 34 Iacomi F, Purica M, Budianu E, Prepelita P & Macovei D, *Thin Solid Films*, 515 (2007) 6080.
- 35 Tong X L, Jiang D S, Yan QY, Hu W B, Liu Z M & Luo M Z, *Vacuum*, 82 (2008) 1411.
- 36 Ullrich B, Ariza-Flores D & Bhowmick M, *Thin Solid Films*, 558 (2014) 24.
- 37 D Kaushik, R R Singh, M Sharma, D K Gupta, N P Lalla, & R K Pandey, *Thin Solid Films*, 515 (2007) 7070.
- 38 Abdolazadeh Z A & Ghodsi F E, *Sol Energy Mater Sol Cells*, 105 (2012) 249.
- 39 Foster N F, *J Appl Phys*, 38 (1967) 149.
- 40 Dresner J & Shallcross F V, *J Appl Phys*, 34 (1963) 2390.
- 41 Singh V, Singh B P, Sharma T P & Tyagi R C, *Opt Mater*, 20 (2002) 171.
- 42 Singh B P, Singh V, Tyagi R C & Sharma T P, *Appl Surf Sci*, 254 (2008) 2233.
- 43 Wang Z D, Yoshida M & George B, *Comp Theor Chem*, 1017 (2013) 91.
- 44 Wang S, Gao Q & Wang J, *J Phys Chem B*, 109 (2005) 17281.
- 45 Timchenko V P, Novozhilov A L & Slepysheva O A, *J Gen Chem*, 74 (2004) 1046.
- 46 Singh B P, Kumar R, Kumar A & Tyagi R C, *Mater Res Express*, 2 (2015) 106401.
- 47 Bilgin V, Kose S, Atay F & Akyuz I, *Mater Chem Phys*, 94 (2005) 103.
- 48 Post B, *X-Ray Spectrom*, 4 (1975) A18.
- 49 Huang B, Yang Y, Chen X & Ye D, *Catal Commun*, 11 (2010) 844.
- 50 Jassim S A J, Zumaila A A R A & Waly G A A Al, *Res Phys*, 3 (2013) 173.
- 51 Orlianges J C, Champeaux C, Dutheil P, Catherinot A & Mejean T M, *Thin Solid Films*, 519 (2011) 7611 .
- 52 Tauc J, *Amorphous and liquid semiconductors*, Edited by J Tauc, (Springer US, Boston, MA), (1974) 159.